Journal of Thermal Engineering
Web page info: https://jten.yildiz.edu.tr
DOI: 10.18186/thermal.1189093

Research Article

Evaluation and optimization of single-effect vapour absorption system for the dairy industry using design of experiment approach

Alka SOLANKI[1*], Yash PAL[2]

[1]*School of Renewable Energy and Efficiency , National Institute of Technology Kurukshetrate, India*
[2]*Department of Electrical Engineering, National Institute of Technology, Kurukshetra, India*

ARTICLE INFO

Article history
Received: 5 December 2020
Accepted: 15 February 2021

Keywords:
Single Effect Vapour Absorption System; RSM; ANOVA; COP; Optimization; Design of Experiments; Dairy Industry; Process Heat Applications

ABSTRACT

Several investigations have emphasized process parameters of single-effect vapour absorption system; yet, the influence of process parameters on thermodynamic performance of the absorption system has not been focussed for the best performance conditions. Several process parameters such as absorber, generator, evaporator, and condenser temperatures influence an absorption refrigeration system's exergetic and energetic performance. In the present study, the design of experiments has been used for the optimization of process parameters. A 1.5 kW cooling capacity of the LiBr-H_2O absorption system has been developed and tested under various operating conditions. Performance characteristics such as in COP and heat dissipated by the condenser (Q_c) of the ARS system have been studied at different ranges of operating parameters. For the process parameter optimization, a central composite design under Response Surface Methodology has been used. The maximum COP and Q_c have been obtained as 0.827 and 2488.79, respectively at optimum values of generator temperature (T_g) = 95.1 °C, condenser temperature (T_c) = 45.3 °C, absorber temperature (T_a) = 28.4 °C and evaporator temperature (T_e) =15 °C. The optimum conditions obtained by the design of experiments have been validated through experiments on the ARS system, and experiments have been conducted at closer conditions of the optimized values of the operating parameters and found the maximum COP and Q_c as 0.926 and 2518.01, respectively. The results of this paper have been very useful in designing a better vapour absorption system.

Cite this article as: Solanki A, Pal Y. Evaluation and optimization of single-effect vapour absorption system for the dairy industry using design of experiment approach. J Ther Eng 2022;8(5):619–631.

***Corresponding author.**
*E-mail address: alkasolanki10@gmail.com, yashpal@nitkkr.ac.in

This paper was recommended for pub lication in revised form b y Regional editor Liu Yang

Published by Yıldız Technical University Press, İstanbul, Turkey

INTRODUCTION

The Indian dairy industry is one of the fastest-growing industries in the world. The demand for dairy products is rising progressively because of the increase in population and their lifestyle. The increase in dairy products demand also increased energy demand during the last two decades by Desai et al. [1]. More energy consumption resulted in more CO_2 emissions. Oza et al. and Sharma et al. advise the use of renewable energy should be encouraged [2,19]. Renewable energy sources are one of the alternatives and the only solution for growing industries urge by Owusu et al. [3] and Mustafa et al. [23]. The dairy industries can use renewable energy to improve efficiency and reduce energy consumption in process heat applications Guiney et al. [4] and Ansari [24]. The integration of a vapour absorption system in process heat applications in the dairy industry can provide energy-efficient opportunities. Using such technology towards savings in electricity can replace the existing designs in process heat applications. The collective savings of energy in the chilling process and hot water generation may significantly affect the economy of the entire dairy plant. Canbolat et al. [5] conducted the parametric optimisation of absorption refrigeration systems and obtained COP and eCOP of the system as 0.6255 and 0.289, respectively. Oza et al. [2] optimized a 3 TR ammonia-water absorption system using Taguchi method and found the maximum COP at the low condenser and higher evaporator temperature. Lu et al. [6] optimised the heat-driven absorption refrigeration system and found the optimal COP as 0.86 at T_g = 60°C and T_e = 5 °C. Iffa et al. [7] optimised different configurations of absorption refrigeration systems operated with many refrigerant pairs using the design of experiments. Parham et al. [8] optimised the absorption chiller cycle based on COP. The performance of the absorption chiller working with H_2O + LiCl was compared with the absorption chiller functioning with LiBr + H_2O. The results indicated that the performance of the absorption chiller working with LiBr + H_2O was higher than that of the absorption chiller working with H_2O + LiCl at optimal conditions. Manu et al. [9] optimised the performance parameters of the LiBr+H_2O absorption refrigeration system using Taguchi towards maximum COP. Mashayekh et al. [10] obtained the optimum working conditions of absorption chillers. The worked-out optimum conditions can be used as a theoretical guide for further studies on the absorption chillers. Micallef [11] presented a linear model of absorption systems Omar and Micallef [12] developed a mathematical model of the absorption refrigeration system provided with an absorber. The results obtained from the mathematical model of the absorption refrigeration system can be used in designing and sizing such systems. Abbaspour et al. [13] found the optimal values of design parameters in a LiBr+H_2O absorption system. Costa et al. [14] fitted a quadratic polynomial model to COP and parameter settings towards optimum cycle efficiency. Anderson et al. [15] simulated the performance of four types of solar collectors with regard to their suitability for heating and cooling in the dairy industry. Finally, it is concluded that both flat plate and evacuated tube-based solar collector systems have better performance and make it sincere contribution to energy saving in the dairy industry. Sandey et al. [16] concluded that the solar energy could be used in the dairy industry for solar drying, for pumping dairy fluid, for room conditioning, for cold storage of milk & milk products, for lighting and electric fencing. Aphornratana and Sriveerakul [17] described an experimental investigation of a single-effect absorption using aqueous lithium–bromide as working fluid. A 2 kW cooling capacity experimental refrigerator was tested with various operating temperatures. It was found that the solution circulation ratio (SCR) has a strong effect on the system performance. The measured SCR was 2–5 times greater than the theoretical prediction. This was due to the low performance of the absorber. The use of solution heat exchanger could increase the COP by up to 60%. Meraj et al. [18] developed the thermal modelling of solar milk pasteurization system operated through N number of fully covered semi-transparent photovoltaic thermal integrated parabolic concentrator. It is also concluded that the proposed pasteurization system under optimal design and operating parameters can produce 216 kg of pasteurized milk and 5.7 kW h of electrical energy. Correspondingly, after simulation it is inferred that the proposed system is self-sustained under 6 h of operation. Meraj et al. [19] analysed proposed system was analysed under the constant mass flow rate of collectors fluid. Mathematical expressions have also been derived for generator temperature of the absorption unit as a function of both design and operating parameters. Azhar et al. [20] presented internal irreversibility at each component of a single-effect vapour absorption refrigeration system. Results show that for a single tube, UA value in the system component ranges from 2.99 W/K to 48.9 W/K depending on the operating conditions and design parameters of the system.

The refrigeration system's performance is influenced by various parameters such as temperatures of condenser, generator, absorber, and evaporator. Nonetheless, less work has been reported in the open literature on optimization of single-effect vapour absorption system for the dairy industry to get maximum performance in terms of COP and heat recovery in the condenser for process heat application using the design of experiments approach. Thus, the main objective of this study is to optimize the performance of a vapour absorption system for a dairy industry using the design of experiments approach. So, the dairy industry can utilise a vapour absorption system for less energy consumption.

DESIGN OF EXPERIMENTS USING RESPONSE SURFACE METHODOLOGY

Response Surface Methodology

RSM (Response Surface Methodology) is a statistical tool used to model and analyse multivariate systems [15]. The connection between the dependent and independent variables is commonly unknown. RSM is often used to approximate the response in terms of predictive variables accordingly. The mathematical model of the second-order polynomial response surface can be expressed as:

$$Y = F(X1, X2, X3, \ldots\ldots Xn) + \square \quad (1)$$

Here, Y is the answer, ☐ is the error term, Xi (1, 2, 3 ... ... n) are process variables. Function F is generally a second, third, fourth or even higher-order polynomial operation. A quadratic polynomial and is written as:

$$y = \beta_0 + \sum_{i=1}^{n} \beta_i X_i + \sum_{i=j}^{n} \sum \beta_{i,j} X_i X_j + \sum_{i=1}^{n} \beta_{ii} X_i^2 + \square \text{ [15]} \quad (2)$$

where, β_o presents unknown polynomial coefficients. By the least-squares method, these unknown coefficients β_i(i = 0, 1, 2, . . . n) are calculated. In this study, four parameters are considered for optimising the absorption refrigeration system, such as evaporator temperature, generator temperature, absorber temperature, and condenser temperature, as shown in Table 1. The levels of parameters are chosen based on the literature review.

A series of experiments was conducted in the experimental plan to study the impact of parameters to obtain the relationship between variables based on selected parameters and their levels. At the operating temperatures, the mass flow rate at sate point 1,2,3 = 8.852 kg/s, at point 4,5,6 = 7.852 and point 7,8,9 and 10 = 1kg/s.

The impact of generator temperature, absorber temperature, evaporator temperature on system COP and heat rejection in the condenser is optimized using RSM. Using various instruments such as standard probability plots, residual analysis, etc., the adequacy of models is checked.

Analysis of Variance (ANOVA)

The ANOVA is used to determine the percentage of contribution of every parameter on the performance characteristics, as it is a statistical approach. The ANOVA determines the order of impacting factors on the response. The impacts of each parameter on the COP and heat recovery in the condenser are examined. The significance level of the statistical analysis is 0.05, corresponding to a 95% confidence interval. The F-test has also been carried out for the reliability of outcomes. The parameter is considered statistically significant if the F-test value is greater than F-value.

Table 1. Parameters and their operation levels

Sr. No.	Input parameters	Level 1	Level 2
1	Generator temperature(T_g) °C	95.0	140.0
2	Condenser temperature(T_c) °C	40.0	90.0
3	Absorber temperature(T_a) °C	20.0	45.0
4	Evaporator temperature(T_e) °C	6.0	24.0

Mathematical Model

A single-effect vapour absorption cogeneration sys-tem model has been developed, as shown in Figure 1. The system comprises a condenser, absorber, solution heat exchanger (SHE), evaporator, solution expansion valve, refrigerant heat exchanger (RHE), pump and refrigerant expansion valve.

Fig. 1 shows the schematic of the vapour absorption cogeneration system. The cycle has two circuits: the refrigerant circuit (7-11) and LiBr–H_2O solution circuit (1-6). Heat is transferred to the generator (Q_g), which evaporates the refrigerant H_2O at high pressure (P_c); the evaporated H_2O is then convected to the condenser (7). The condenser dissipates heat (Q_c), and then H_2O changes phase from vapour to liquid (8).

Then, the refrigerant H_2O is conducted to refrigerant expansion valve (RTV) via a refrigerant heat exchanger to reach evaporation pressure (P_c); consequently, it leads to the evaporator (10). The cooling process is conducted in the evaporator once the refrigerant soaks up (Q_e) from the environment; this causes the refrigerant to evaporate once again (11) and then lead to the absorber, where it combines with the weak solution coming from the generator. Once it mixes up, a LiBr-H_2O solution with a low concentration is formed and release heat (Q_a). After that, the solution is pumped to the generator (3) until it reaches condenser

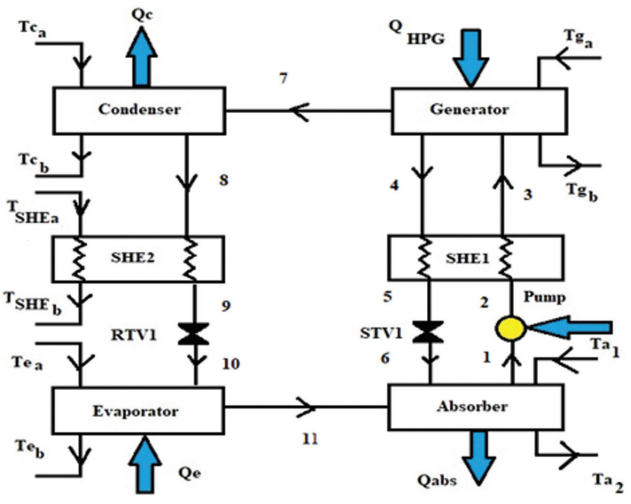

Figure 1. Schematic of the vapour absorption system.

pressure (P_c) via a solution heat exchanger, increasing solution temperature.

The cycle initiates after getting sufficient temperature in the generator. A part of the refrigerant evaporates and goes to the condenser (7). The rest of the solution with high concentration is fed to the heat exchanger (4) here, its temperature is decreased. Then it is passed by a throttle valve (STV), where its pressure is reduced to the evaporation pressure (P_e).

The fundamental equations utilized in the study of the first law of thermodynamics are represented here:

$$\sum m_i - \sum m_o = 0 \tag{3}$$

$$\sum m_i X_i - \sum m_o X_o = 0 \tag{4}$$

Here, m is the mass flow rate and

X is the mass fraction of LiBr in the solution.

By using the equation (3) and (4), the mass balancing of such elements of the absorption system has been advanced as:

By estimating is the coefficient of performance (COP), the whole performance of the absorption system has been calculated as:

$$COP = \frac{Q_e}{Q_{HTG} + W_p} \tag{5}$$

Here, W_p is the pump work, Q_e is the refrigerant effect, and Q_{HTG} is the heat rate in the generator.

RESULTS AND DISCUSSION

Optimization Using RSM

In the first step, to determine the impact of process parameters on the COP and heat recovery in the condenser, the RSM method has been applied. The COP and heat recovery in the condenser is estimated from the experimental work. The COP of the system and Q_c are found for each operating parameter value as suggested by the design expert software V 12 and shown in Table 2. 28 runs have different parameters.

From the above table, it is inferred that experiments have been performed as per the design of experiments along with a different combination of parameters value.

The multiple regression analysis has provided the following equations, based on the design of experiments analysis:

$$\begin{aligned} COP = {} & +0.6955 + 0.0759 \times T_g - 0.3808 \times T_c - 0.4338 \\ & \times T_a - 0.4275 \times T_e - 0.1323 \times T_g \times T_c - 0.3654 \\ & \times T_g \times T_a + 0.9587 \times T_g T_e - 0.0266 \times T_c T_a - 0.0051 \\ & \times T_c T_e + 0.1291 \times T_a T_e \end{aligned} \tag{25}$$

$$\begin{aligned} Q_c = {} & +2435.88 + 41.76 \times T_g - 109.22 \times T_c - 96.31 \\ & \times T_a - 25.02 \times T_e - 9.19 \times T_g \times T_c - 97.38 \times T_g \\ & \times T_a + 32.06 \times T_g \times T_e + 10.29 \times T_c T_a + 48.94 \\ & \times T_c T_e - 94.32 \times T_a T_e \end{aligned} \tag{26}$$

ANOVA for RSM model

The analysis of variance of both the models of COP and Q_c have been shown in Tables 3 and 4, respectively.

Probability tests and F tests were performed to verify the suitability of the model. To study the significance of each coefficient, p-values are used, which also reveal the strength of interaction of each variable. A lower value of p shows the greater meaning of the corresponding coefficient. The F-test results are automatically verified by the software and estimate the probability of all terms of the regression equation. It

Table 2. CCD design matrix for COP and Q_c obtained through DOE

Tg	Tc	Ta	Te	COP	Qc
95	40	22	15	0.8927	2510
140	90	30	15	0.6404	2382
117.5	65	32.5	15	0.7564	2447
117.5	65	32.5	15	0.7564	2447
117.5	65	32.5	15	0.7564	2447
140	89	32.5	24	0.6987	2386
117.5	65	45	6	0.2922	2447
95	65	25	15	0.7053	2403
117.5	40	40	24	0.4023	2337
140	45	45	15	0.4378	2382
117.5	65	45	6	0.6922	2447
140	90	20	6	0.6243	2382
95	40	32.5	15	0.9023	2447
140	90	29	18	0.6704	2510
117.5	65	32.5	15	0.7564	2403
95	40	29	15	0.8795	2510
95	65	32.5	15	0.5987	2403
95	40	45	15	0.9013	2510
117.5	88	31	13	0.2933	2346
117.5	86.5	27	14	0.4584	2353
95	77	32.5	15	0.526	2351
125	92	32.5	14	0.3778	2343
124	94.5	32.5	14	0.2085	2330
117.5	82	29.5	15	0.5941	2373
96	79.5	27	17	0.3632	2342
98	75	30	14	0.1663	2366
100	87	31	11	1.304	2316
123	103	29	17	0.1819	2289

Table 3. ANOVA of RSM model for COP

Source	Sum of Squares	df	Mean Square	F-value	p-value	
Model	1.18	10	0.1178	2.86	0.0273	significant
A-Tg	0.0275	1	0.0275	0.6686	0.4249	
B-Tc	0.4253	1	0.4253	10.33	0.0051	
C-Ta	0.1493	1	0.1493	3.63	0.0739	
D-Te	0.2632	1	0.2632	6.4	0.0216	
AB	0.0407	1	0.0407	0.9882	0.3341	
AC	0.1371	1	0.1371	3.33	0.0856	
AD	0.4848	1	0.4848	11.78	0.0032	
BC	0.0007	1	0.0007	0.0163	0.8998	
BD	0	1	0	0.0005	0.9825	
CD	0.0062	1	0.0062	0.1495	0.7039	
Residual	0.6996	17	0.0412			
Lack of Fit	0.6196	13	0.0477	2.38	0.2083	not significant
Pure Error	0.08	4	0.02			
Cor Total	1.88	27				

Table 4. ANOVA of RSM model for Q_c

Source	Sum of Squares	df	Mean Square	F-value	p-value	
Model	92694.7	10	9269.47	10.93	< 0.0001	significant
A-Tg	8324.56	1	8324.56	9.81	0.0061	
B-Tc	34987.08	1	34987.1	41.24	< 0.0001	
C-Ta	7357.74	1	7357.74	8.67	0.0091	
D-Te	901.68	1	901.68	1.06	0.317	
AB	196.03	1	196.03	0.2311	0.6369	
AC	9735.09	1	9735.09	11.48	0.0035	
AD	542.36	1	542.36	0.6393	0.435	
BC	100.46	1	100.46	0.1184	0.735	
BD	1879.56	1	1879.56	2.22	0.1549	
CD	3284.36	1	3284.36	3.87	0.0656	
Residual	14421.4	17	848.32			
Lack of Fit	12969.4	13	997.65	2.75	0.17	not significant
Pure Error	1452	4	363			
Cor Total	1.07E+05	27				

is significant if the probability is greater than the proposed model, it is less than 0.005. As shown in Table 3 and 4, the F value of 3.07 for COP and F value of 10.93 for heat rejection in the condenser Q_c can be seen. The p values of the models of COP and Q_c can also seen from Tables 3 and 4 as less than 0.0001. The condenser temperature T_c has a big impact on the COP in this case. Some of the significant terms of the model are T_g, T_c, T_e, $T_g \times T_a$, $T_c \times T_e$ and $T_a \times T_e$, in addition to the ANOVA results. The term T_e^2 has the greatest effect on Q_c, in the case of heat dissipation from the condenser. Fig. 2 and 3 are the normal residual plots for COP and Q_c, which reveal the studentized residuals with a percentage of general probability, respectively.

Effects of the Operating Variables

The effects of various operating parameters on the COP and heat dissipated by the condenser have been shown graphically in Figs. 4 to 15. The graphs have been generated using Design-Expert software.

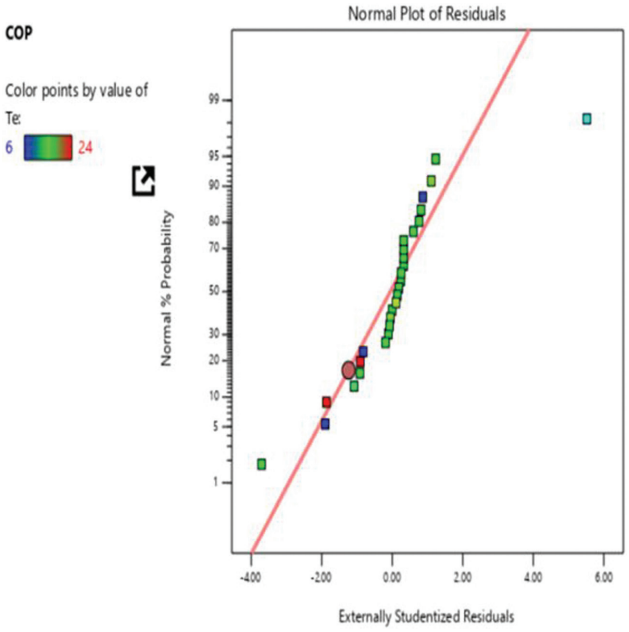

Figure 2. Normal plot of residuals for COP.

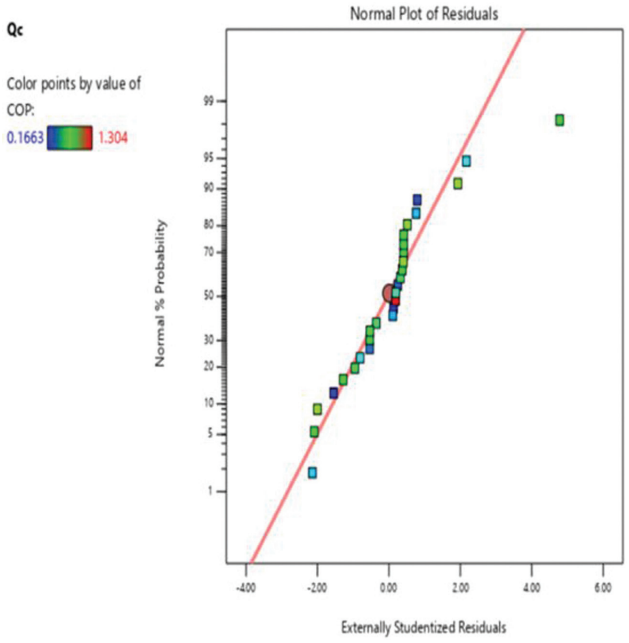

Figure 3. Normal plot of residuals for Q_c.

Optimum conditions predicted by RSM

The optimum parameters towards maximum COP and Q_c are forecasted by implementing RSM technique using design expert software, as shown in Table 6. The optimum values of parameters for maximum COP and Q_c are T_g = 95.1°C, T_c = 45.3°C, T_a = 28.4°C and T_e =15.0°C. The predicted COP and Q_c at optimum parameters are 0.853 and 2488.79 kW, respectively.

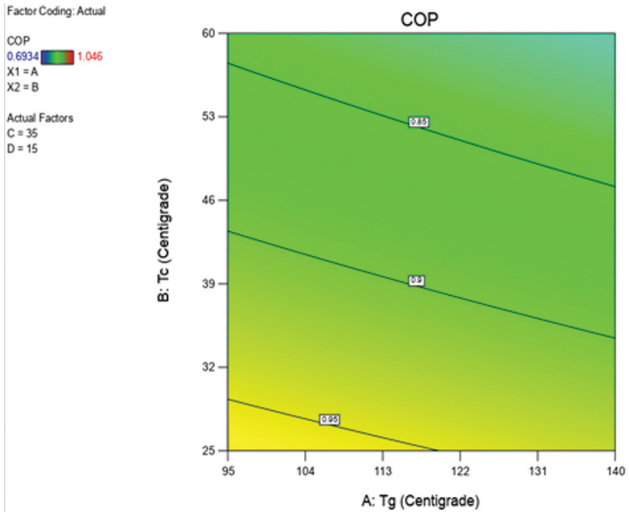

Figure 4. Effect of T_g and T_c on COP.

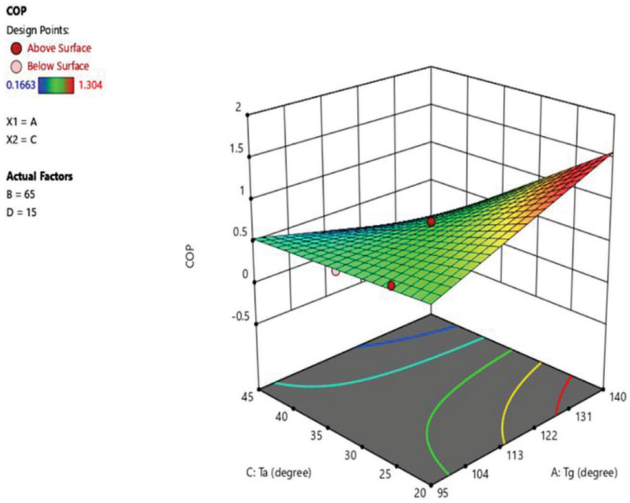

Figure 5. Effect of T_g and T_a on COP.

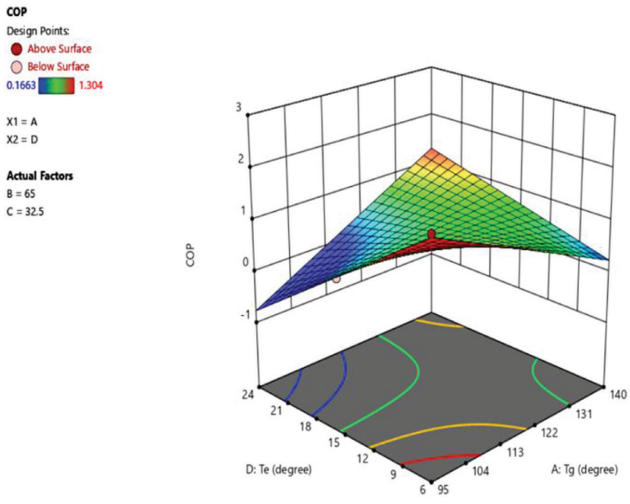

Figure 6. Effect of T_g and T_e on COP.

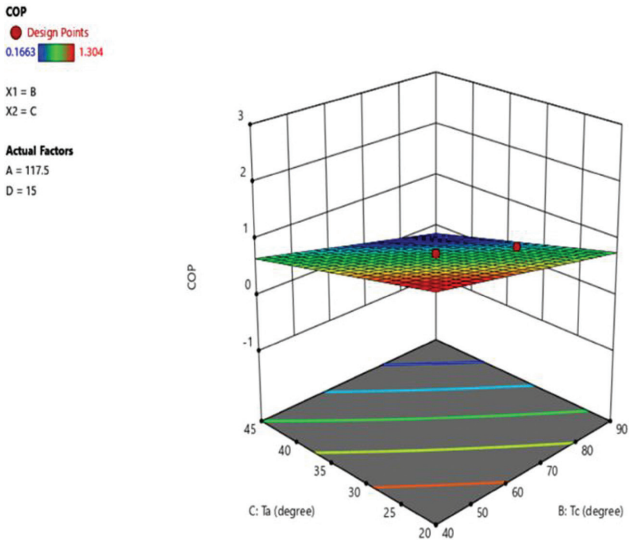

Figure 7. Effect of T_a and T_c on COP.

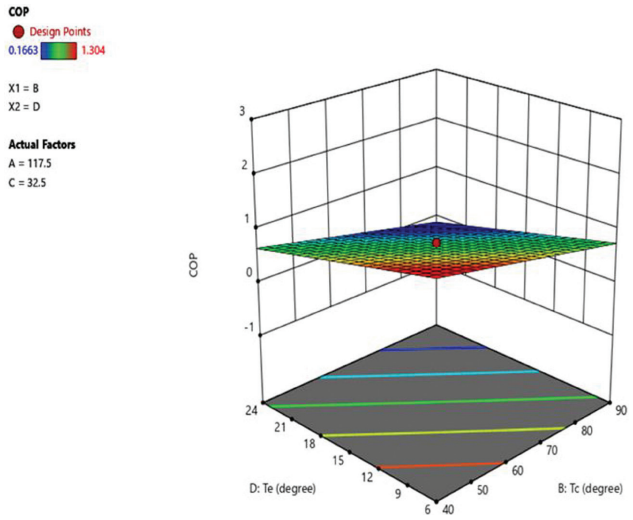

Figure 8. Effect of T_e and T_c on COP.

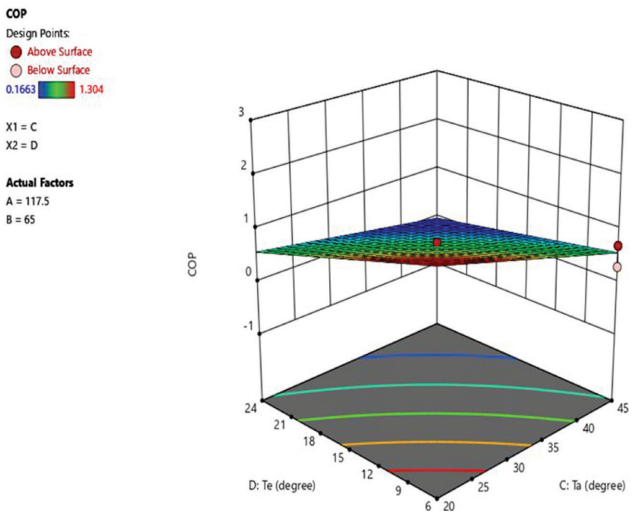

Figure 9. Effect of T_a and T_e on COP.

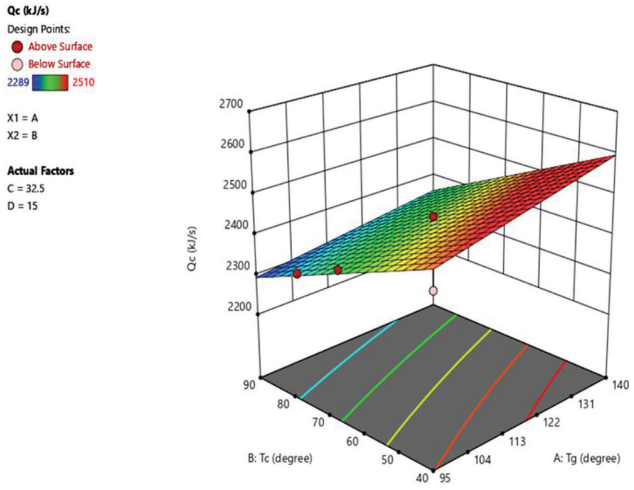

Figure 10. Effect of T_g and T_c on Q_c.

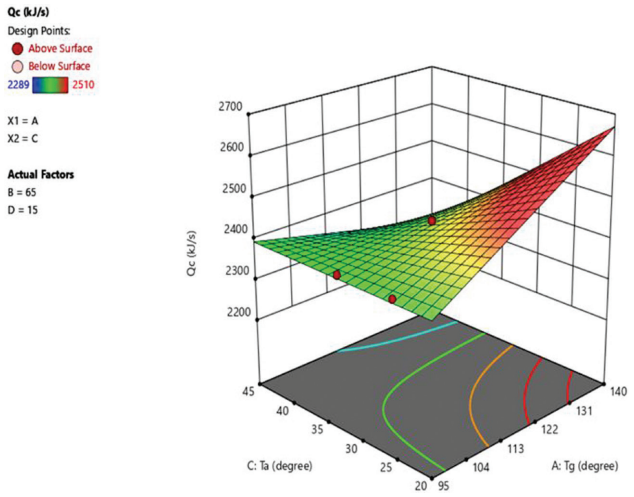

Figure 11. Effect of T_g and T_a on Q_c.

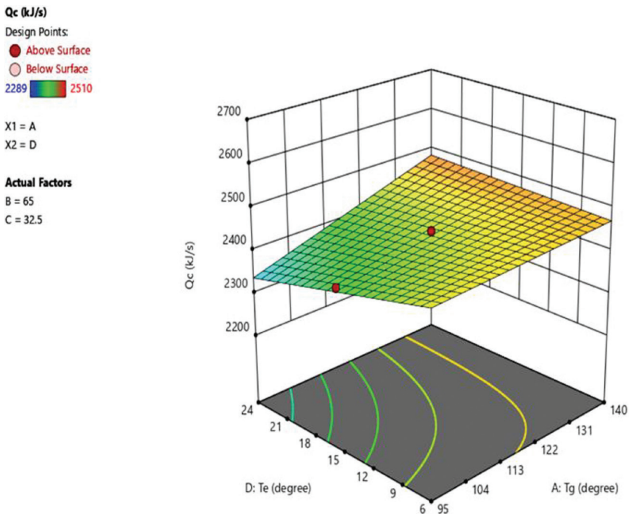

Figure 12. Effect of T_g and T_e on Q_c.

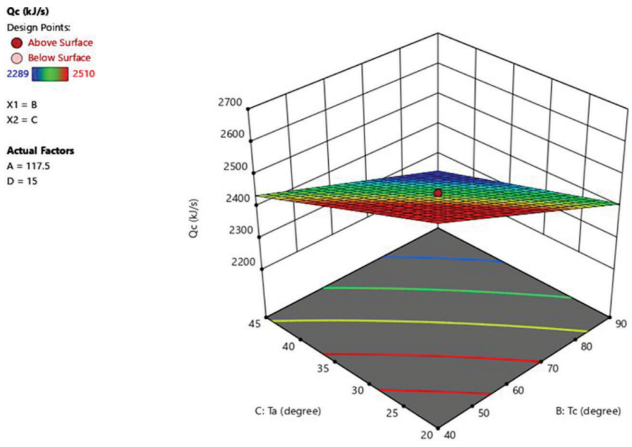

Figure 13. Effect of T_a and T_c on Q_c.

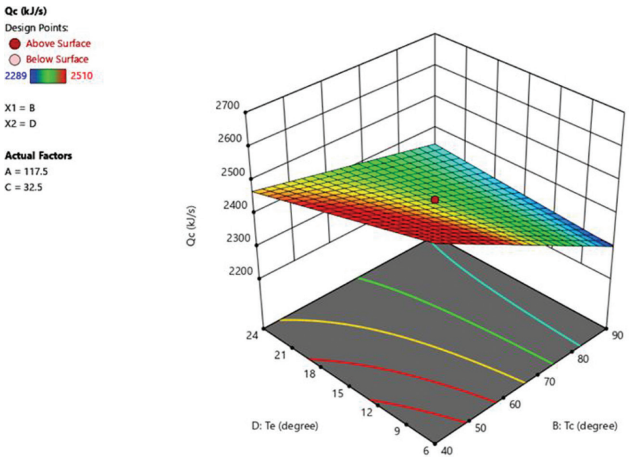

Figure 14. Effect of T_e and T_c on Q_c.

The above table shows that for 10 experimental runs, optimized COP and Q_c are given.

Experimental validation of the predicted model by RSM

An experimental set-up with a cooling capacity of 1.5 kW has been developed for the feasibility assessment of its applicability in the dairy industry. The test facility has been shown schematically in fig. 16.

All the four seamless vessels used as evaporator, condenser, generator and absorber have been made of copper. In the generator, baffle plates have been provided at the upper end to get the pool boiling and avoid liquid solution droplets going out with water vapours. The evaporator has been designed like a spray column to ensure maximum heat transfer in the present case.

The absorber used in the experimental facility act as a falling film column. The solution has been made to spray over a cooling coil in the absorber to form a liquid film over the coil to get maximum heat transfer in the present case.

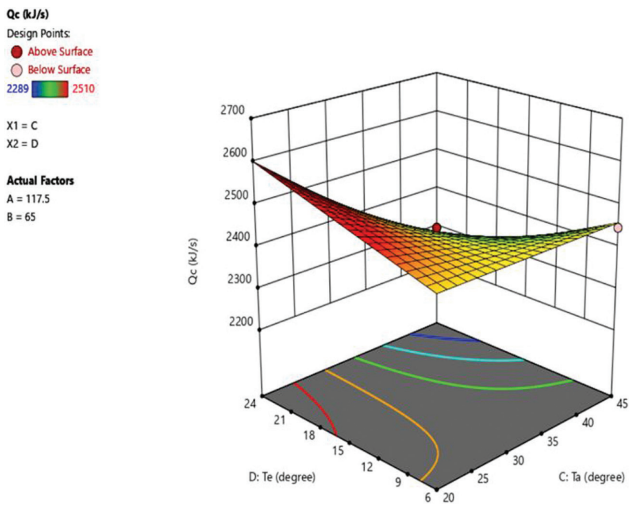

Figure 15. Effect of T_e and T_a on Q_c.

Table 5. Optimization solution predicted by DOE

Sr. No	T_g	T_c	T_a	T_e	COP	Q_c	Desirability
1	95.1	45.3	28.4	15.0	0.827	2488.79	1
2	119.9	87.6	24.3	14.4	0.721	2343.17	1
3	117.5	82.0	29.5	15.0	0.520	2371.48	1
4	95.0	65.0	32.5	15.0	0.571	2416.53	1
5	117.5	86.5	27.0	14.0	0.626	2343.96	1
6	140.0	90.0	20.0	6.0	0.739	2386.30	1
7	95.0	65.0	25.0	15.0	0.676	2389.91	1
8	96.0	79.5	27.0	17.0	0.182	2342.36	1
9	98.0	79.0	27.4	13.7	0.714	2334.82	1
10	107.7	77.5	32.3	11.4	0.788	2372.73	1

Table 6. The details of the measuring instruments

Sr. No	Measuring Instruments	Range	Resolutions	Parameters
1	Hydrometer	0.990-1.170	0.01	Specific gravity
2	J-Type thermocouple	0-600 °C	0.1 °C	Temperature
4	Pressure gauge	0-30 psi	0.5 psi	Pressure

The solution heated up with the help of ETC in the generator, and the cold solution from the absorber has been made to in counter current directions via the annular duct and the inner tube, respectively.

A bypass flow control valve has been employed at the inlet of the heat exchanger to measure the heat

Figure 16. (I) Experimental test rig, (II) Evacuated tube collector used to get the required generator temperature and (III) Internal views of the generator, condenser, evaporator and absorber.

Table 7. The detailed specifications of the ETC collector

Material of Glass	Borosilicate Glass
Thickness of Glass Tube	Outer tube thickness: 1.8 mm, inner tube thickness: 1.6 mm
Inner diameter	47 mm
Outer diameter	58 mm
Coefficient of Thermal Expansion	3.3×10^{-6}/K
Vacuum rate	$P \leq 5.0\times10^{-4}$Pa
Recommended operating pressure	0.2 kg/cm^2
Stagnation Parameter	$Y \geq 290$ M^2 °C/kW
Selective coating type	AIN/AIN-SS/CU – Sputtering
Value of absorptance and emittance of the black coating	Absorptance: $\alpha \geq 93.5\%$, Emission rate: $\varepsilon \leq 5\%$

exchanger effectiveness. Voltage and current transducers have been used for measuring supply power. The cooling water flow rates across the condenser and the absorber have been controlled with the help of solenoid control valves. All of the vessels used as the main components of the vapour absorption system were provided with sight-glasses to observe inside liquid levels. Infra-red switches have been employed on the sight glasses to measure the fluid levels. In the steady-state condition, the liquid volume has been measured using sight-glass over a finite time interval.

The performance of the practical mechanism has been analysed using experimental observations taken above a linear-state processing time of 60 minutes. The experimental outcomes have been recorded by varying the absorber temperatures, generator, condenser and evaporator.

Further, the details of the measuring instruments have been given in Table 6.

To verify the accuracy of the predicted model, experiments have been performed over very close values of the optimized parameters as shown in Table 7. The experiments have been conducted on the test facility developed at NISE Gurugram, India, as shown in Fig. 16. The best experimental observations of COP and Q_c as 0.926 and 2518.01 kW, respectively, have been in close approximation with the optimized values of COP and Q_c. The plots of predicted vs actual, residuals vs predicted, and residuals vs run are shown in Fig. 18-23.

Figure 17. Photographic view of the Evacuated Tube Collector used in the experiment.

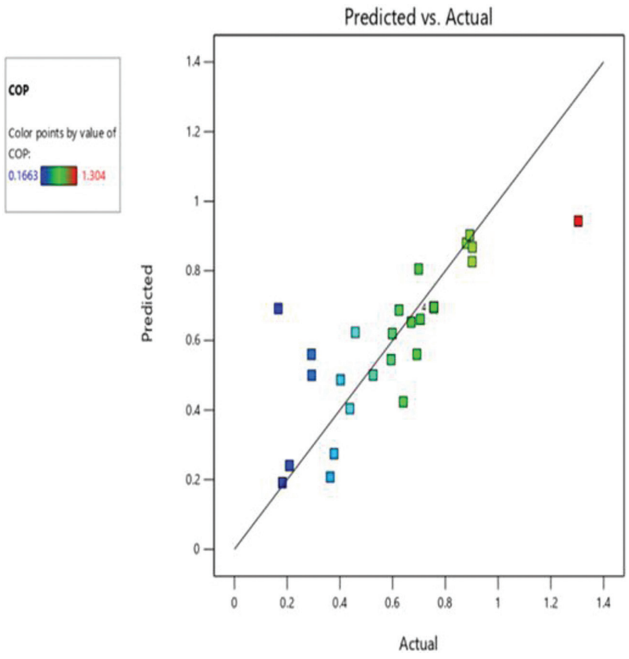

Figure 18. Predicted vs actual plot for COP.

Table 8. Experimental observations close to the predicted optimized parameters

Sr. No	T_g	T_c	T_a	T_e	COP	Q_c
1	95.0	40.0	22.0	15.0	0.926	2518.01
2	99.9	84.3	34.3	11.9	0.712	2340.04
3	101.0	65.0	29.0	16.0	0.620	2400.00
4	93.0	66.0	30.0	15.0	0.700	2415.00
5	110.0	71.0	28.0	14.0	0.683	2406.00

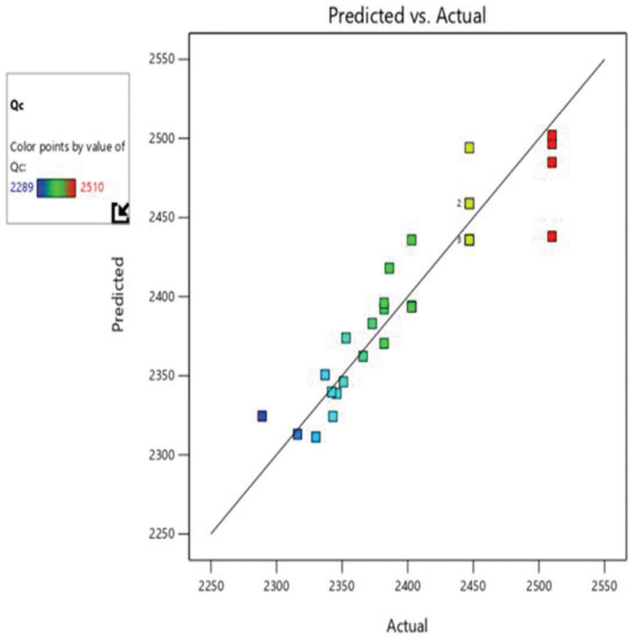

Figure 19. Predicted vs actual plot for Q_c.

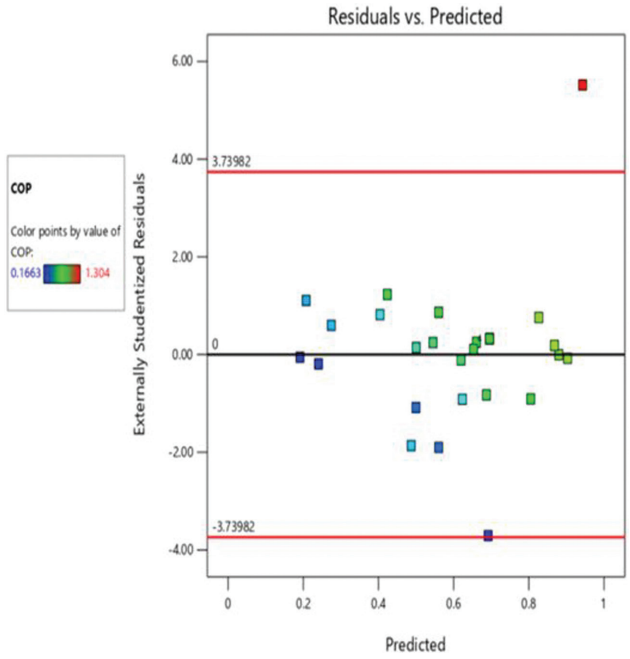

Figure 20. Residuals vs predicted plot for COP.

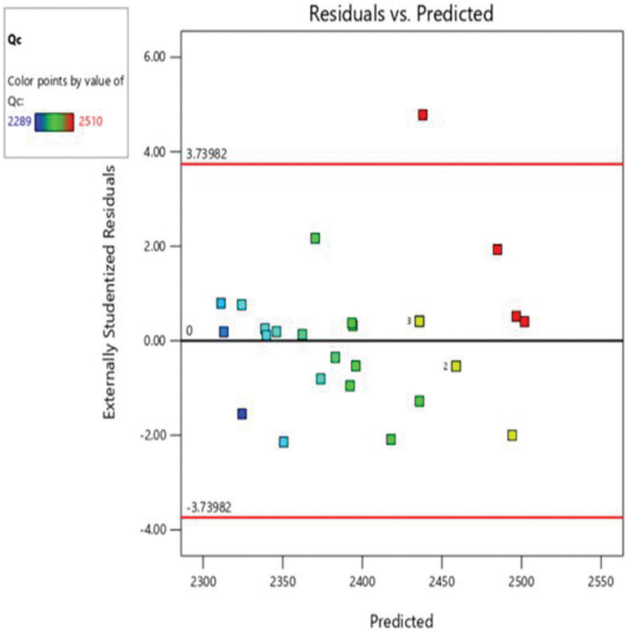

Figure 21. Residuals vs predicted plot for Q_c.

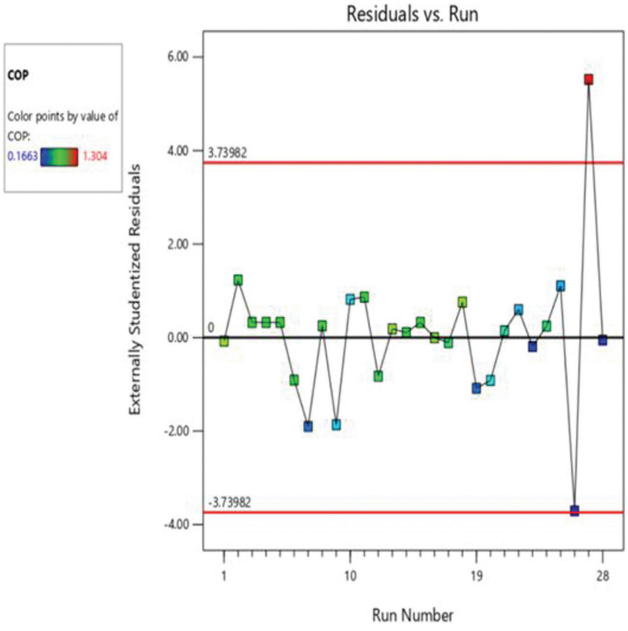

Figure 22. Residuals vs run plot for COP.

CONCLUSION

In this study, the RSM technique optimises process parameters for a single-effect vapour absorption system so that the dairy industry can utilise a single effect vapour absorption system operating at best-operating conditions. The maximum COP of 0.926 was obtained experimentally at temperatures at the generator, condenser, absorber and evaporator as T_g = 95.1 °C, T_c = 45.3 °C, T_a = 28.4 °C and T_e =15.0 °C, respectively and was in good agreement with the optimized COP. Further, the maximum Q_c was obtained as 2518.01 kW, and the evaporator load is 2349 kW at the same optimal conditions. The experimentally validated optimum conditions have been suggested to be very useful in designing a better vapour absorption system.

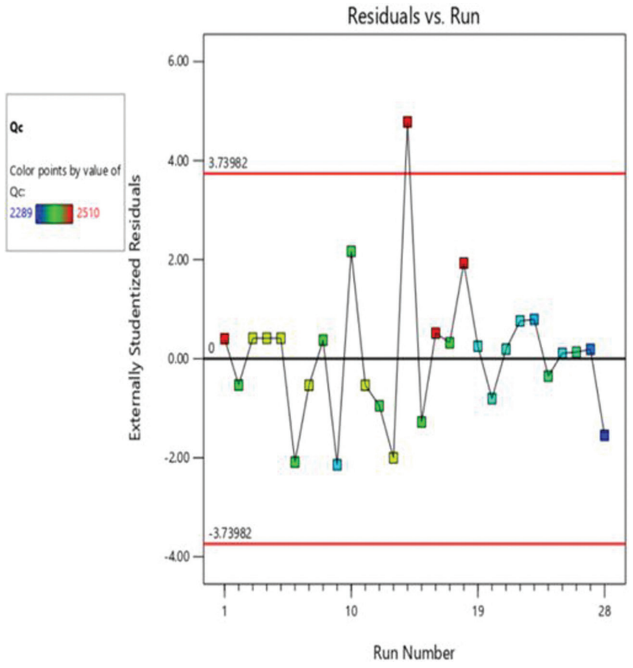

Figure 23. Residuals vs run plot for Q_c.

ACKNOWLEDGEMENT

The authors oblige the recognition of the experimental test facility given through the National Institute of Solar Energy (NISE), Gurugram, India.

AUTHORSHIP CONTRIBUTIONS

Authors equally contributed to this work.

DATA AVAILABILITY STATEMENT

The authors confirm that the data that supports the findings of this study are available within the article. Raw data that support the finding of this study are available from the corresponding author, upon reasonable request.

CONFLICT OF INTEREST

The author declared no potential conflicts of interest with respect to the research, authorship, and/or publication of this article.

ETHICS

There are no ethical issues with the publication of this manuscript.

NOMENCLATURE

Symbols and abbreviations

ANOVA	Analysis of variance
COP	Coefficient of performance
DOE	Design of experiment
EES	Engineering equation solver
LiBr	Lithium bromide
$\dot{m}$	Mass flow rate (kg/s)
$\dot{m}_r$	Mass flow rate f refrigerant (kg/s)
P	Pressure (kPa)
Qe	Refrigerating effect (kW)
QG	Heat input of generator
T	Temperature (°C)
Ta	Absorber temperature (°C)
Tb	Boundary temperature (K)
Tc	Condenser temperature (°C)
Te	Evaporator temperature (°C)
Tg	enerator temperature (°C)
X	Concentration of Lithium bromide in solution (%)

Subscripts

a, Abs	Absorber
c	Condenser
D	Destruction
e	Evaporator
g	Generator
Ex.	Expansion
i	Represents, corresponding state points
o	Outlet condition
p	Pump
r	Refrigerant
RTV	Expansion valve
S	Strong
SHE	Solution heat exchanger
STV	Solution throttle valve
W	Weak

REFERENCES

[1] Desai DD, Raol JB, Patel S, Chauhan I. Application of Solar energy for sustainable Dairy Development. Eur J Sustain Dev 2013;2:131–140. [CrossRef]

[2] Oza VH, Bhatt NM. Optimization of ammonia-water absorption refrigeration system using taguchi method of design of experiment. Int J Mech Solids 2018;13:111–126.

[3] Owusu PA, Asumadu-Sarkodie S. A review of renewable energy sources, sustainability issues and climate change mitigation. Cogent Eng 2016;3:1–14. [CrossRef]

[4] Guiney W. Pasteurization and Refrigeration for Milk and Dairy Products. 2018. https://www.thomasnet.com/insights/pasteurization-and-refrigeration-for-milk-and-dairy-products-/.

[5] Canbolat AS, Bademlioglu AH, Arslanoglu N, Kaynakli O. Performance optimization of absorption refrigeration systems using Taguchi, ANOVA and Grey Relational Analysis methods. J Clean Prod 2019;229:874–885. [CrossRef]

[6] Lu Y, Roskilly AP, Ma C. A techno-economic case study using heat driven absorption refrigeration technology in UK industry. Energy Procedia 2017;123;173–179. [CrossRef]

[7] BenIffa R, Bouaziz N, Kairouani L. Optimization of absorption refrigeration systems by design of experiments method. Energy Procedia 2017;139;280–287. [CrossRef]

[8] Parham K, Atikol U, Yari M, Agboola, OP. Evaluation and optimization of single stage absorption chiller using (LiCl + H2O) as the working pair. Adv Mech Eng 2013;2013:683157. [CrossRef]

[9] Manu S, Chandrashekar TK, Girisha C. Optimization lithium bromide (LiBr)–water absorption refrigeration using taguchi for low capacity. Indian J Sci Technol 2016;9:1–4. [CrossRef]

[10] Mashayekh H, Salehi GR, Taghdiri E, Hamedi MH. Thermo-economic Optimization of Absorption Chiller Cycle. Proc. World Renew. Energy Congr – Sweden 2011;8–13;1497–1504. [CrossRef]

[11] Micallef D, Micallef C. Mathematical model of a vapour absorption refrigeration unit. Int J Simul Model 2010;9:86–97. [CrossRef]

[12] Osta-Omar SM, Micallef C. Mathematical model of a Lithium-Bromide/water absorption refrigeration system equipped with an adiabatic absorber. Computation 2016;4:44. [CrossRef]

[13] Razmi AR, Arabkoohsar A, Nami H. Thermoeconomic analysis and multi-objective optimization of a novel hybrid absorption/recompression refrigeration system. Energy 2019;210:118559. [CrossRef]

[14] Ricardo Costa N, Garcia J. Applying design of experiments to a compression refrigeration cycle. Cogent Eng. 2015;2:992216. [CrossRef]

[15] Rajneesh, Kumar R. Enhancement in evaporative effectiveness of an evaporative tubular heat dissipator using experimental design approach. Heat Transf - Asian Res 2016;45:144–162. [CrossRef]

[16] Ketfi O, Merzouk M, Merzouk NK, Metenani S. Performance of a Single Effect Solar Absorption Cooling System (Libr-H2O). Energy Procedia 2015;74;130–138. [CrossRef]

[17] Kaushik SC, Arora A. Energy and exergy analysis of single effect and series flow double effect water-lithium bromide absorption refrigeration systems. Int J Refrig 2009;32:1247–1258. [CrossRef]

[18] Modi A, Prajapat R. Pasteurization process energy optimization for a milk dairy plant by energy audit approach. Int J Sci Technol Res 2014;3:181–188.

[19] Mohan M, Sharma VK. Studies on thermodynamic performance of three stage sorption heat transformer. Appl Therm Eng 2019;154:228–237. [CrossRef]

[20] Meraj MD, Mahmood SM, Khan ME, Azhar MD, Tiwari GN. Effect of N-Photovoltaic thermal integrated parabolic concentrator on milk temperature for pasteurization: A simulation study. Renew Energy 2021;163:2153–2164. [CrossRef]

[21] Meraj M, Khan ME, Azhar M. Performance analyses of photovoltaic thermal integrated concentrator collector combined with single effect absorption cooling cycle: constant flow rate mode. J Energy Res Technol 2020.;142:1–28. [CrossRef]

[22] Ansari KA, Azhar M, Siddiqui A. Exergy analysis of single-effect vapor absorption system using design parameters. J Energy Res Technol 2020;143:4048594. [CrossRef]

[23] Mustafa AA, Noranai Z, Imran AA. Solar absorption cooling systems: A review. J Therm Eng 2021;7: 970–983. [CrossRef]

[24] Ansari NA, Arora A, Gautam S, Manjunath K. Optimum parametric analysis based on thermodynamic modeling of a compression absorption cascade refrigeration system. J Therm Eng 2020;6:559–576. [CrossRef]